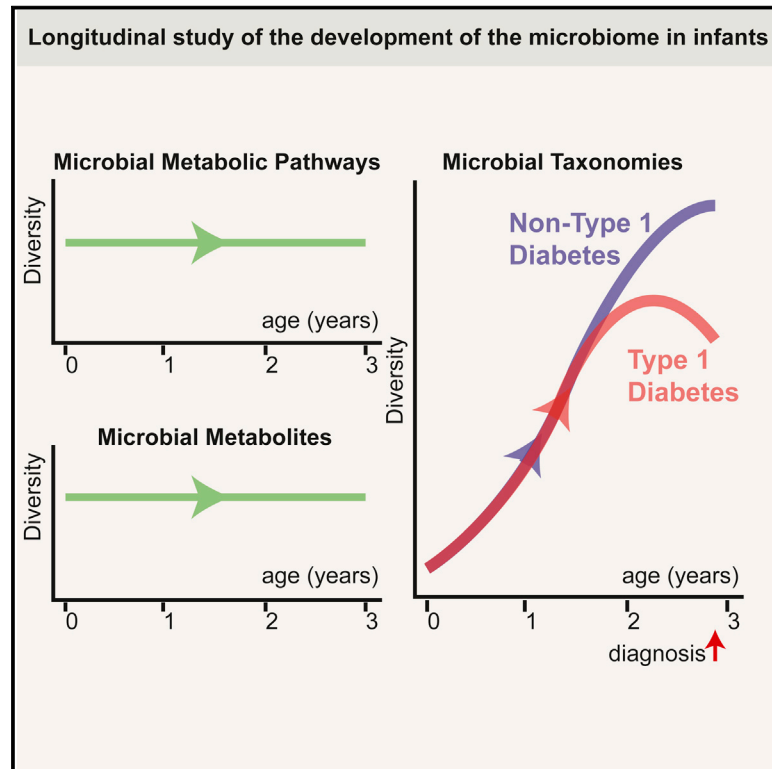


# Cell Host & Microbe

## The Dynamics of the Human Infant Gut Microbiome in Development and in Progression toward Type 1 Diabetes

### Graphical Abstract



### Authors

Aleksandar D. Kostic, Dirk Gevers, ..., Mikael Knip, Ramnik J. Xavier

### Correspondence

xavier@molbio.mgh.harvard.edu

### In Brief

Kostic et al. perform a microbiome analysis of type 1 diabetes (T1D), examining the infant gut microbiome as T1D develops. Microbial metabolic pathways remain remarkably stable throughout infancy. T1D onset is preceded by a drop in community diversity and a spike in inflammation-associated species and metabolic pathways.

### Highlights

- Gut microbial metabolic pathways but not taxonomies are stable throughout infancy
- Strain composition of high-abundance species remains constant throughout infancy
- Decreased community diversity occurs after seroconversion but before onset of T1D
- T1D onset is preceded by increased inflammation-associated organisms and pathways



# The Dynamics of the Human Infant Gut Microbiome in Development and in Progression toward Type 1 Diabetes

Aleksandar D. Kostic,<sup>1,2,3</sup> Dirk Gevers,<sup>1</sup> Heli Siljander,<sup>4,5</sup> Tommi Vatanen,<sup>1,6</sup> Tuulia Hyötyläinen,<sup>7,11</sup> Anu-Maaria Hämäläinen,<sup>9</sup> Aleksandr Peet,<sup>10</sup> Vallo Tillmann,<sup>10</sup> Päivi Pöhö,<sup>8,11</sup> Ismo Mattila,<sup>7,11</sup> Harri Lähdesmäki,<sup>6</sup> Eric A. Franzosa,<sup>3</sup> Outi Vaarala,<sup>5</sup> Marcus de Goffau,<sup>12</sup> Hermie Harmsen,<sup>12</sup> Jorma Ilonen,<sup>13,14</sup> Suvi M. Virtanen,<sup>15,16,17</sup> Clary B. Clish,<sup>1</sup> Matej Orešič,<sup>7,11</sup> Curtis Huttenhower,<sup>1,3</sup> Mikael Knip,<sup>4,5,18,19,23</sup> on behalf of the DIABIMMUNE Study Group,<sup>22</sup> and Ramnik J. Xavier<sup>1,2,20,21,23,\*</sup>

<sup>1</sup>Broad Institute of MIT and Harvard, Cambridge, MA 02142, USA

<sup>2</sup>Center for Computational and Integrative Biology, Massachusetts General Hospital and Harvard Medical School, Boston, MA 02114, USA

<sup>3</sup>Department of Biostatistics, Harvard School of Public Health, Boston, MA 02115, USA

<sup>4</sup>Children's Hospital, University of Helsinki and Helsinki University Hospital, 00290 Helsinki, Finland

<sup>5</sup>Research Program Unit, Diabetes and Obesity, University of Helsinki, 00290 Helsinki, Finland

<sup>6</sup>Department of Information and Computer Science, Aalto University School of Science, 02150 Espoo, Finland

<sup>7</sup>Steno Diabetes Center, 2820 Gentofte, Denmark

<sup>8</sup>Faculty of Pharmacy, University of Helsinki, 00290 Helsinki, Finland

<sup>9</sup>Department of Pediatrics, Jorvi Hospital, 02740 Espoo, Finland

<sup>10</sup>Department of Pediatrics, University of Tartu, Estonia and Tartu University Hospital, 51014 Tartu, Estonia

<sup>11</sup>VTT Technical Research Centre of Finland, 02044 Espoo, Finland

<sup>12</sup>Department of Medical Microbiology, University Medical Center Groningen and University of Groningen, 9713 GZ Groningen, the Netherlands

<sup>13</sup>Immunogenetics Laboratory, University of Turku, 20520 Turku, Finland

<sup>14</sup>Department of Clinical Microbiology, University of Eastern Finland, 70211 Kuopio, Finland

<sup>15</sup>Department of Lifestyle and Participation, National Institute for Health and Welfare, 00271 Helsinki, Finland

<sup>16</sup>School of Health Sciences, University of Tampere, 33014 Tampere, Finland

<sup>17</sup>Science Centre, Pirkanmaa Hospital District, 33521 Tampere, Finland

<sup>18</sup>Folkhälsan Research Center, 00290 Helsinki, Finland

<sup>19</sup>Department of Pediatrics, Tampere University Hospital, 33521 Tampere, Finland

<sup>20</sup>Gastrointestinal Unit and Center for the Study of Inflammatory Bowel Disease, Massachusetts General Hospital and Harvard Medical School, Boston, MA 02114, USA

<sup>21</sup>Center for Microbiome Informatics and Therapeutics, Massachusetts Institute of Technology, Cambridge, MA 02139, USA

<sup>22</sup>Mikael Knip, Katriina Koski, Matti Koski, Taina Härkönen, Samppa Ryhänen, Heli Siljander, AnuMaaria Hämäläinen, Anne Ormiston, Aleksandr Peet, Vallo Tillmann, Valentina Ulich, Elena Kuzmicheva, Sergei Mokurov, Svetlana Markova, Svetlana Pylova, Marina Isakova, Elena Shakurova, Vladimir Petrov, Natalya V. Dorshakova, Tatyana Karapetyan, Tatyana Varlamova, Jorma Ilonen, Minna Kiviniemi, Kristi Ainek, Helis Janson, Raivo Iibo, Tiit Salum, Erika von Mutius, Juliane Weber, Helena Ahlfors, Henna Kallionpää, Essi Laajala, Riitta Lahtesmaa, Harri Lähdesmäki, Robert Moulder, Viveka Öling, Janne Nieminen, Terhi Ruotula, Outi Vaarala, Hanna Honkanen, Heikki Hyöty, Anita Kondrashova, Sami Oikarinen, Hermie J.M. Harmsen, Marcus C. De Goffau, Gjal Welling, Kirsi Alahuhta, Tuuli Korhonen, Suvi M. Virtanen, and Taina Öhman.

<sup>23</sup>Co-senior author

\*Correspondence: [xavier@molbio.mgh.harvard.edu](mailto:xavier@molbio.mgh.harvard.edu)  
<http://dx.doi.org/10.1016/j.chom.2015.01.001>

## SUMMARY

Colonization of the fetal and infant gut microbiome results in dynamic changes in diversity, which can impact disease susceptibility. To examine the relationship between human gut microbiome dynamics throughout infancy and type 1 diabetes (T1D), we examined a cohort of 33 infants genetically predisposed to T1D. Modeling trajectories of microbial abundances through infancy revealed a subset of microbial relationships shared across most subjects. Although strain composition of a given species was highly variable between individuals, it was stable within individuals throughout infancy. Metabolic composition and metabolic pathway abundance re-

mained constant across time. A marked drop in alpha-diversity was observed in T1D progressors in the time window between seroconversion and T1D diagnosis, accompanied by spikes in inflammation-favoring organisms, gene functions, and serum and stool metabolites. This work identifies trends in the development of the human infant gut microbiome along with specific alterations that precede T1D onset and distinguish T1D progressors from non-progressors.

## INTRODUCTION

The initial colonization of the human gut microbiota begins in utero (Aagaard et al., 2014) and is strongly influenced by

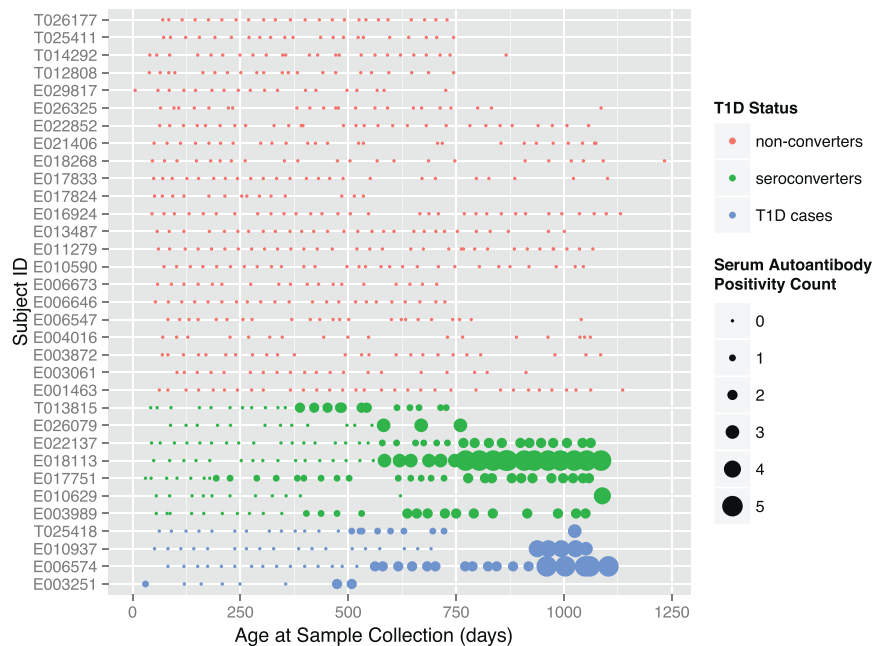


**Figure 1. A Cohort to Assess the Dynamics of the Developing Human Gut Microbiota in Infancy**

Individuals are represented in rows, and each point is a stool sample. The size of the points represents the number of serum autoantibodies (0–5) that were positive at the time of the sample collection. See also Figure S1.

stream of multiple Toll-like receptors involved in microbial sensing, in the NOD mouse results in complete protection from diabetes (Wen et al., 2008). Further, heterozygous MyD88<sup>KO/+</sup> NOD mice, which normally develop robust disease, are protected from diabetes when exposed from birth to the gut microbiota of a MyD88-KO NOD donor (Wen et al., 2008). Therefore, disease progression in the NOD mouse is driven in part by an exaggerated innate immune response to symbiotic microbiota, and altering the composition of the microbiota can curtail

microbial exposures at birth (Dominguez-Bello et al., 2010). The initial seeding and development of this community may have long-term physiological consequences. Low-resolution longitudinal studies in 14 infants (Palmer et al., 2007) and higher-resolution studies in a single infant (Koenig et al., 2011) have documented the gradual increase in phylogenetic diversity, nonrandom community assembly, the effects of introducing table foods, and the large taxonomic shifts that can occur during infancy. High-resolution multi'omic studies that examine the dynamics of infant gut microbiome development in a large, longitudinal cohort have been lacking, though one recent study has shown that children with severe acute malnutrition exhibit decreased “microbiota maturity” using such a cohort (Subramanian et al., 2014). Events in early microbiome development may have a role in promoting susceptibility to or protection from disease later in life; this has been demonstrated in mice (Cho et al., 2012; Cox et al., 2014), and it may also be true for type 1 diabetes (T1D) (Brown et al., 2011; Giongo et al., 2011; de Goffau et al., 2013).

T1D is an autoimmune disorder that results from T cell-mediated destruction of the insulin-producing  $\beta$  cells of the pancreatic islets. Although approximately 70% of T1D cases carry predisposing HLA risk alleles, only 3%–7% of children with those alleles develop T1D (Achenbach et al., 2005), suggesting a significant nongenetic component to the disease. The incidence of T1D has been increasing rapidly over the past few decades, particularly in the youngest age groups (0–4 years) (Harjutsalo et al., 2008), suggesting a significant nongenetic component to the disease. The incidence of T1D is particularly high in Finland, where 1 in 120 children develop T1D before 15 years of age (Knip et al., 2005).

Although there have been limited human studies of the microbiome in T1D to date, the notion that T1D pathogenesis may be influenced by microbial exposures has been well established in murine models. The knockout of MyD88, an adaptor down-

this response and prevent disease. Prospective studies are required to assess whether the microbiota is similarly involved in human T1D progression; however, such cohorts are exceedingly difficult to build (Brown et al., 2011; Giongo et al., 2011).

Here, we assess the composition of the gut microbiota in a densely sampled, prospective, longitudinal cohort of 33 HLA-matched infants followed from birth until 3 years of age. We use this unprecedented sample resolution to describe the dynamics and stability of the developing microbiome in the infant gut of an at-risk T1D cohort. We show that although there are significant shifts in taxonomic composition over time, the relative abundance of metabolic pathways within individuals remains remarkably constant throughout infancy. We identify a 25% drop in alpha-diversity in children who progress to T1D compared to controls, which occurs after seroconversion but before disease diagnosis, and identify alterations to both the phylogenetic and metabolic pathway composition of the microbiome during this time that is characteristic of a proinflammatory environment. Our results demonstrate significant alterations to the gut microbiome in T1D progressors prior to disease onset.

## RESULTS

### Extensive Characterization of the Infant Gut Microbiota in a Longitudinal Cohort

To characterize the development of the infant gut microbiome and the relationship between the gut microbiota and islet autoimmunity and progression to T1D, we assembled a prospective, longitudinal collection of stool samples from infants at risk for disease (Figure 1). Infants from Finland and Estonia were recruited at birth based on HLA risk genotyping (Table 1 and see Table S1 available online). Parents collected their infants' stool at approximately monthly intervals. The cohort was comprised of 33 infants, 11 of whom seroconverted to serum autoantibody positivity (referred to hereafter as “seroconverters”; defined as

**Table 1. Summary of Study Cohort**

Subject ID	Country of Origin	T1D Status	HLA Type	Autoantibody Positive	Age at Seroconversion (Days)	Age at T1D Diagnosis (Days)
T026177	Estonia	nonconverter	DQB1*0302/*0501-DRB1*0401	N/A	N/A	N/A
T025411	Estonia	nonconverter	DQB1*0302/*0501-DRB1*0404	N/A	N/A	N/A
T014292	Estonia	nonconverter	DQA1*05/*03-DQB1*02/*0301	N/A	N/A	N/A
T012808	Estonia	nonconverter	DQA1*05/*0201-DQB1*02/*02	N/A	N/A	N/A
E029817	Finland	nonconverter	DQB1*0302/*04-DRB1*0404	N/A	N/A	N/A
E026325	Finland	nonconverter	DQB1*0302/*0501-DRB1*0404	N/A	N/A	N/A
E022852	Finland	nonconverter	DQB1*0302/*0501-DRB1*0404	N/A	N/A	N/A
E021406	Finland	nonconverter	DQB1*0302/*0302-DRB1*0401/*0401	N/A	N/A	N/A
E018268	Finland	nonconverter	DQB1*0302/*0604-DRB1*0404	N/A	N/A	N/A
E017833	Finland	nonconverter	DQA1*05-DQB1*02/*04	N/A	N/A	N/A
E017824	Finland	nonconverter	DQB1*0302/*0604-DRB1*0404	N/A	N/A	N/A
E016924	Finland	nonconverter	DQA1*05-DQB1*02/*04	N/A	N/A	N/A
E013487	Finland	nonconverter	DQA1*05/*03-DQB1*02/*0302-DRB1*0401	N/A	N/A	N/A
E011279	Finland	nonconverter	DQB1*0302/*04-DRB1*0404	N/A	N/A	N/A
E010590	Finland	nonconverter	DQB1*0302/*04-DRB1*0401	N/A	N/A	N/A
E006673	Finland	nonconverter	DQA1*05/*03-DQB1*02/*0302-DRB1*0401	N/A	N/A	N/A
E006646	Finland	nonconverter	DQB1*0302/*0501-DRB1*0401	N/A	N/A	N/A
E006547	Finland	nonconverter	DQB1*0302/*0501-DRB1*0404	N/A	N/A	N/A
E004016	Finland	nonconverter	DQB1*0302/*0502-DRB1*0404	N/A	N/A	N/A
E003872	Finland	nonconverter	DQB1*0302/*0501-DRB1*0404	N/A	N/A	N/A
E003061	Finland	nonconverter	DQB1*0302/*0502-DRB1*0405	N/A	N/A	N/A
E001463	Finland	nonconverter	DQB1*0302/*04-DRB1*0401	N/A	N/A	N/A
T013815	Estonia	seroconverter	DQA1*05/*0201-DQB1*02/*02	IAA, GADA	350.4	N/A
E026079	Finland	seroconverter	DQB1*0302/*04-DRB1*0401	IAA, GADA	580.35	N/A
E022137	Finland	seroconverter	DQB1*0302/*0501-DRB1*0401	IAA, GADA, IA-2A, ZNT8A, ICA	562.1	N/A
E018113	Finland	seroconverter	DQB1*0302/*04-DRB1*0401	IAA, GADA, IA-2A, ZNT8A, ICA	587.65	N/A
E017751	Finland	seroconverter	DQA1*05-DQB1*02/*0604	IAA, ICA	175.2	N/A
E010629	Finland	seroconverter	DQB1*0302/*0501-DRB1*0401	IAA, GADA, ZNT8A, ICA	945.35	N/A
E003989	Finland	seroconverter	DQB1*0302/*04-DRB1*0401	IAA, GADA, ZNT8A, ICA	346.75	N/A
T025418	Estonia	T1D case	DQA1*0201/*03-DQB1*02/*0302-DRB1*0404	IAA, GADA, IA-2A, ICA	540.2	879.65
E010937	Finland	T1D case	DQA1*05/*03-DQB1*02/*0302-DRB1*0401	IAA, IA-2A, ZNT8A, ICA	905.2	959.95
E006574	Finland	T1D case	DQB1*0302/*0501-DRB1*0401	IAA, GADA, IA-2A, ZNT8A, ICA	532.9	1,339.55
E003251	Finland	T1D case	DQB1*0302/*0501-DRB1*0401	IAA, GADA, IA-2A, ZNT8A, ICA	357.7	1,168

See also [Table S1](#) and [Table S2](#).

being positive for at least two of the five autoantibodies analyzed in this study; see [Experimental Procedures](#)), and of those, four developed T1D within the time frame of this study (referred to as “T1D cases”; see [Table 1](#) and [Figure 1](#)). The 11 seroconverters were matched with the 22 controls for gender, HLA genotype, and country.

Sequencing of the V4 region of the 16S rDNA gene was carried out on a total of 989 samples using paired-end, partially overlapping reads on the Illumina MiSeq V2 platform as previously described ([Caporaso et al., 2012](#)), yielding a very high depth of

sequencing with a mean of 65,076 reads per sample. Taxonomic profiling was performed using QIIME ([Caporaso et al., 2010](#)), and functional profiling of microbial pathways was inferred from 16S sequences with PICRUSt ([Langille et al., 2013](#)). In total, there were 777 unique samples sequenced by 16S, with a median of 23 unique samples per individual (minimum 8, maximum 34); the full OTU table is available in [Table S2](#). Shotgun metagenomic sequencing was performed on a subset of 124 samples from 19 individuals, including all 11 seroconverters, with a median of 6 samples per individual (minimum 3, maximum 11) ([Figure S1](#)).

The median depth of sequencing was 2.5 Gb per sample. Phylogenetic community profiling of metagenomic data was performed using MetaPhlAn (Segata et al., 2012), and functional profiling of microbial pathways was characterized with HUMAnN (Abubucker et al., 2012).

In addition to 16S and metagenomic sequencing, serum and stool metabolomics were performed on the cohort. For each of the 33 participants, 7 serum samples taken throughout the experimental time frame (Table S1) were subject to metabolomics and lipidomics, and all samples that were used for shotgun metagenomics were also analyzed by stool metabolomics and lipidomics (see Experimental Procedures).

### Gut Microbial Metabolites and Functional Pathways, but Not Taxonomies, Are Stable throughout Infant Development

Principal coordinates analysis of the Bray-Curtis dissimilarity between all 777 16S-sequenced samples revealed that age is the strongest driver of the composition of the infant gut microbiome (Figure 2A). Age accounted for 18% of the variation between samples, and showed a nearly linear gradient diagonally along the first and second principal coordinates. Similarly, the Chao1 alpha-diversity, a measure of the number of distinct microbes in a community, exponentially increased in early development until reaching a maximum at 3 years of age (Figure 2B).

We hypothesized that with increasing taxonomic diversity in the developing gut comes an equivalent change in the metabolic composition of the gut community; however, this was not the case. The stool metabolomics beta-diversity distances between samples did not have as strong of an age trend as did taxonomies (Figure 2C), and the alpha-diversity of stool metabolites was nearly flat across time, with the exception of a few outlier very-early-time point samples that had a much lower diversity (Figure 2D). More strikingly, the relative abundance of metabolic modules in the microbiome remained approximately constant throughout time and across individuals (Figure 2E shows all samples sorted by age across all individuals). Essentially all pathways are encoded by all individuals from the earliest to the latest time points. The evenness is higher in the first few months until it stabilizes (Figure 2F). This may be because the composition of the microbiome requires time to “settle” into its most optimal abundance of functional pathways, which is less evenly distributed than in the earliest time points.

These results demonstrate a remarkable stability in the metabolic pathway coding potential—and the metabolic content—of the microbiome despite dramatic shifts of taxonomic composition throughout human infancy.

### A Model of the Dynamics of the Developing Gut Microbiome

The strength of the age effect in taxonomies and its consistency across individuals suggested that there may be closely shared phylogenetic trajectories that define the development of the gut microbiome, in agreement with previous cross-sectional studies in older children (Yatsunen et al., 2012). To investigate the driving forces behind this effect, we performed pairwise correlations of the trajectories of abundance between all clades

across time on a per-individual basis, excluding T1D cases. Correlations were determined using CCREPE (Faust et al., 2012), a tool designed to find significant correlations in sparse, compositional data such as 16S sequencing data, which are prone to spurious correlations. The Z score for each clade-clade pair was summed across all individuals (excluding T1D cases), revealing a small set of pairs with very strong correlations that were consistent across most subjects. This allowed us to produce a network of the dynamics of the developing gut microbiome (Figure 3). Plotting the corresponding clade abundances over time demonstrates a strongly shared dynamic relationship across time, and across nearly all individuals, for many specific clades in this developmental process. The resulting network at the family level is shown in Figure 3; see Figure S2 for other phylogenetic levels.

### The Infant Gut Microbiome Remains Stable at the Strain Level

Having investigated the dynamics of the infant gut microbiome, we examined its strain-level stability, i.e., the retention of microbial strains across time. Using the shotgun metagenomics data available on 124 samples, we analyzed strain-level markers on a per-species and per-individual basis using MetaPhlAn (Segata et al., 2012). Analysis was restricted to species that have a mean of at least 1× coverage across all time points per individual; 21 species and 12 individuals met this requirement. Using an unweighted discordant marker distance metric (see Supplemental Experimental Procedures), we found that samples were more similar in the intraindividual versus interindividual comparison ( $p < 1e-5$ ; Figure 4A), suggesting that the strain profile for a given species is more similar between samples in a single individual than between samples in two people. Surprisingly, the strain profile remained essentially constant over time for almost all species and in almost all individuals (Figure 4B shows a representative example in which the marker abundance is constant over time (individuals #2 and #3). In a rare case we observed a shift in the strain signature at a specific time point (individual #1). Table S3 shows marker abundances for all individuals with sufficient marker coverage.

We investigated community stability by calculating the Jaccard index, which is defined as the fraction of shared operational taxonomic units (OTUs), between all pairs of samples within an individual in specified time windows (Figure 4C). For instance, we calculated the fraction of shared OTUs within a subject between two samples collected approximately 3 months apart, and found that the Jaccard index is significantly higher than for two samples from the same individual collected 6 months apart. As has been observed in an adult population (Faith et al., 2013), we found that the Jaccard index followed a power-law function (Figure 4C, line). The curve reached an asymptote at a value of approximately 0.1, suggesting that about 10% of bacterial strains (observed here at an OTU-level resolution) were maintained in the infant gut from birth until 3 years of age (Figure 4C). This surprising result demonstrates that although there is tremendous variability in the gut microbiome through infancy, the community at 3 years of age retained a nonnegligible fraction of members that it acquired just after birth.



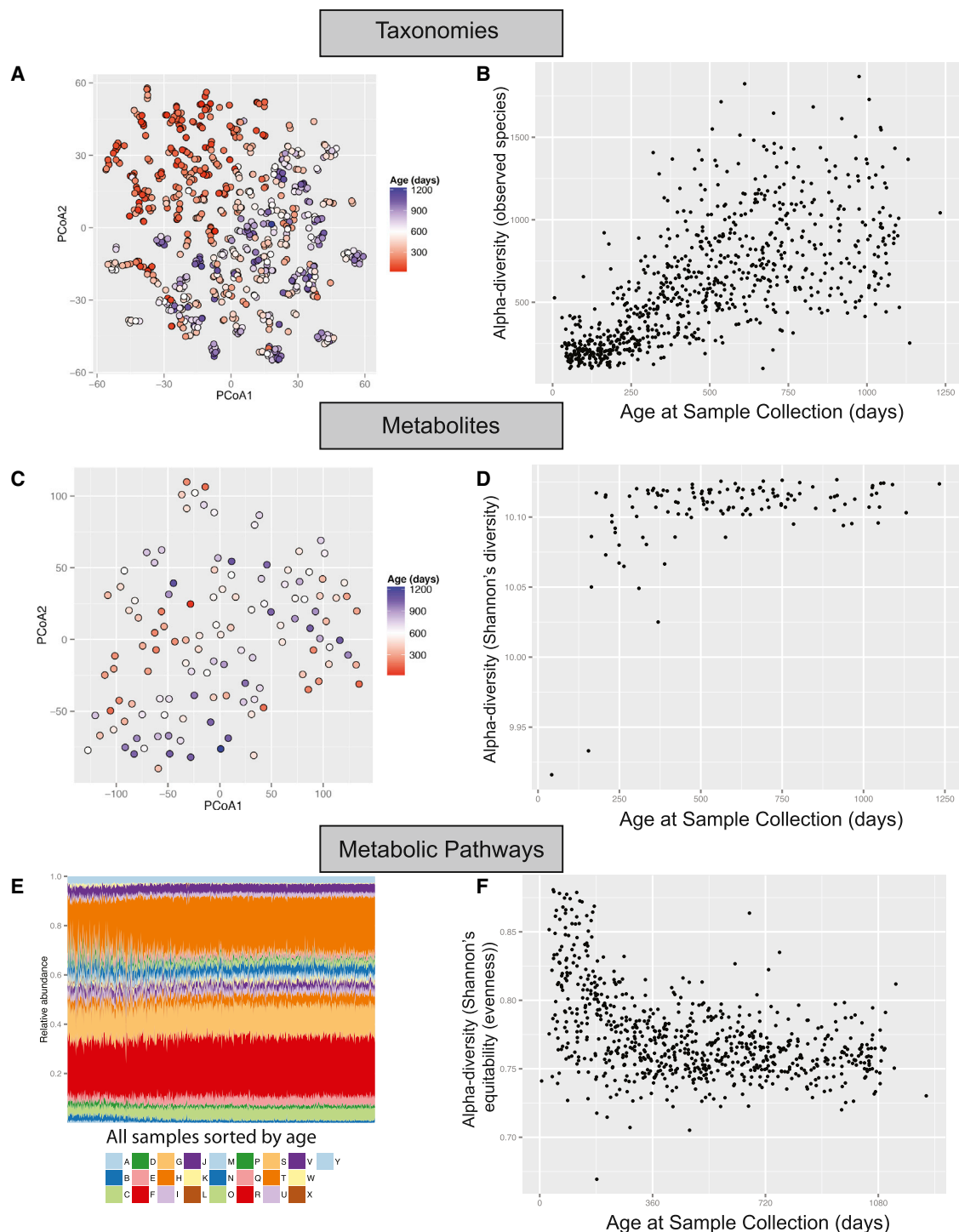


**Figure 2. Gut Microbial Taxonomies Shift Dramatically, whereas Microbial Metabolites and Metabolic Pathways Remain Relatively Stable throughout Infant Development**

(A) Principal coordinates analysis on the unweighted UniFrac distances between samples based on 16S sequencing. Samples are colored by age at stool collection.

(B) Alpha-diversity using the QIIME “observed species” metric on 16S sequencing.

(C) Principal coordinates analysis on stool metabolomics data.

(D) Shannon’s diversity measured on stool metabolomics data.

(E) Bars indicate relative abundances of KEGG metabolic modules: A, aminoacyl tRNA; B, arginine and proline metabolism; C, aromatic amino acid metabolism; D, branched-chain amino acid metabolism; E, carbon fixation; F, central carbohydrate metabolism; G, cofactor and vitamin biosynthesis; H, cysteine and methionine metabolism; I, glyoxylate and glycolate metabolism; J, glutamate metabolism; K, glutamine and glutamate metabolism; L, glutathione metabolism; M, glyoxylate and glycolate metabolism; N, glutamate metabolism; O, glutamine and glutamate metabolism; P, glyoxylate and glycolate metabolism; Q, glutamate metabolism; R, glutamine and glutamate metabolism; S, glyoxylate and glycolate metabolism; T, glutamate metabolism; U, glutamine and glutamate metabolism; V, glyoxylate and glycolate metabolism; W, glutamate metabolism; X, glutamine and glutamate metabolism; Y, glyoxylate and glycolate metabolism.

(legend continued on next page)

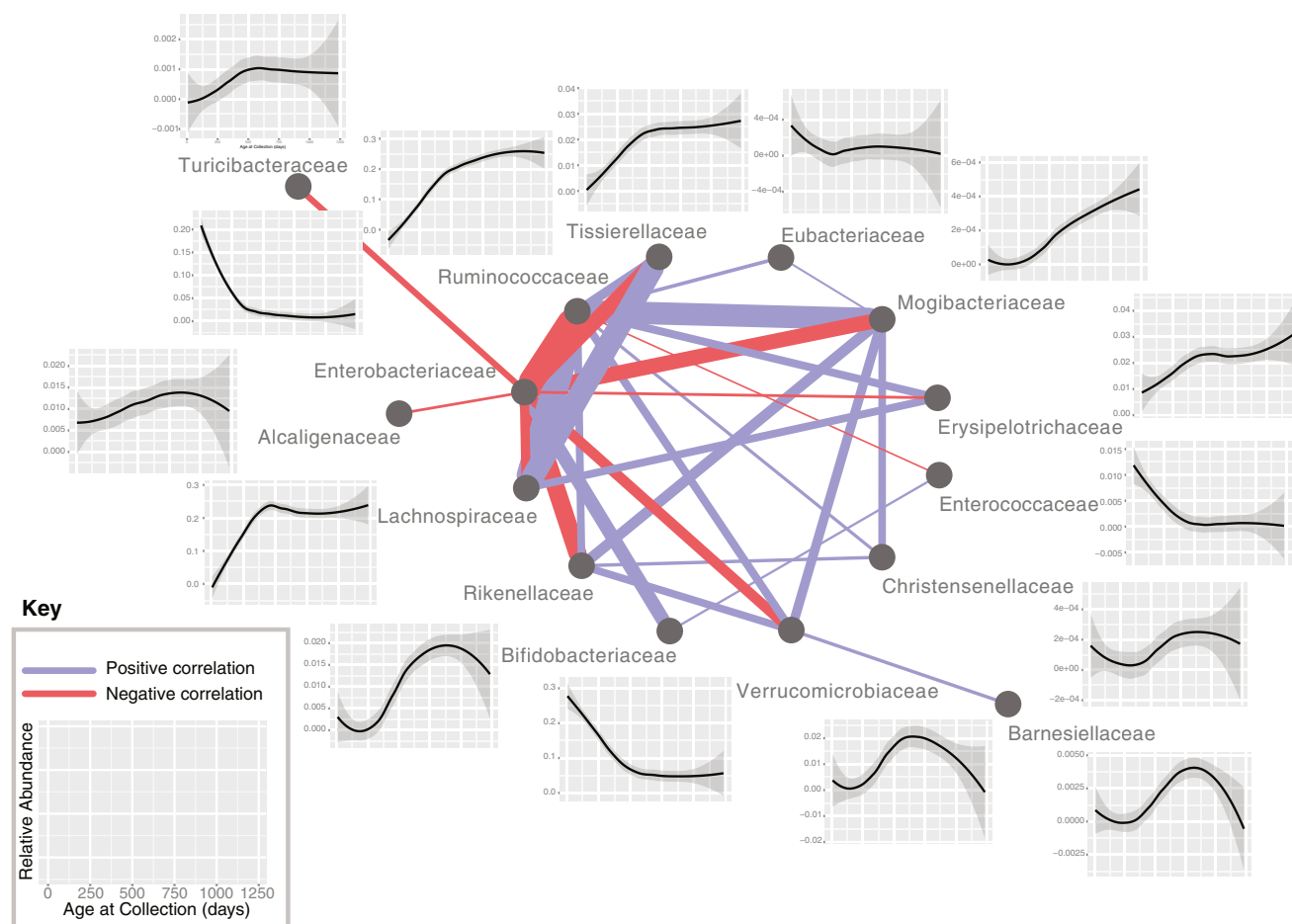


**Figure 3. Temporal Dynamics of Microbial Taxonomies in Infant Gut Development**

Family-level network diagram of the correlation between clades in their trajectories across time, excluding individuals with T1D. Positive correlations are in blue, negative correlations are in red, and the line thickness is proportional to the strength of the correlation (cumulative CREPE Z statistic). The plots show the abundance of the indicated family as a smoothing spline across all healthy individuals with a 95% confidence interval (shaded region). See also Figure S2.

### Correlations between the Gut Microbiome and Diet and Environmental Factors

Extensive metadata relating to both clinical and nonclinical factors were collected for each participant in the study (Table S1), allowing us to assess the association between the gut microbiome and environmental factors in our cohort. To avoid the potential confounding effects of age, multiple sampling from the same individual, and each of the other metadata, all analyses were performed on a reduced set of samples in a limited time frame, using age and other metadata as fixed effects and subject identity as a random effect. This analysis was performed using multivariate association with linear models (MaAsLin) (Morgan et al., 2012), an additive general linear model with boosting that can capture the effects of a parameter of interest while deconfounding the effects of other metadata. This is particularly

important in the current study, as age, diet, and other factors are expected to have strong influences on community composition (Table S1; see Experimental Procedures for the metadata included in the MaAsLin analysis). With MaAsLin, we focused our analysis on a single variable of interest, and systematically “subtracted out” the effect of each of the other potentially confounding metadata variables. A series of five samples from each breastfed subject taken during and after cessation of breastfeeding revealed an increase in *Bifidobacterium* and *Lactobacillus* species during breastfeeding; however, we found that the reduction in Lachnospiraceae was an even stronger effect (Figure S3A). We observed substantial differences between Estonian and Finnish infants, including significantly higher levels of *Bacteroides* and *Streptococcus* species, which contain a number of potential pathobionts, in the Estonians (Figure S3B).

methionine metabolism; I, fatty acid metabolism; J, glycosaminoglycan metabolism; K, histidine metabolism; L, lipid metabolism; M, lipopolysaccharide metabolism; N, lysine metabolism; O, methane metabolism; P, nitrogen metabolism; Q, nucleotide sugar; R, other amino acid metabolism; S, other carbohydrate metabolism; T, polyamine biosynthesis; U, purine metabolism; V, pyrimidine metabolism; W, serine and threonine metabolism; X, sulfur metabolism; and Y, terpenoid backbone biosynthesis.

(F) A measure of evenness of KEGG metabolic modules.

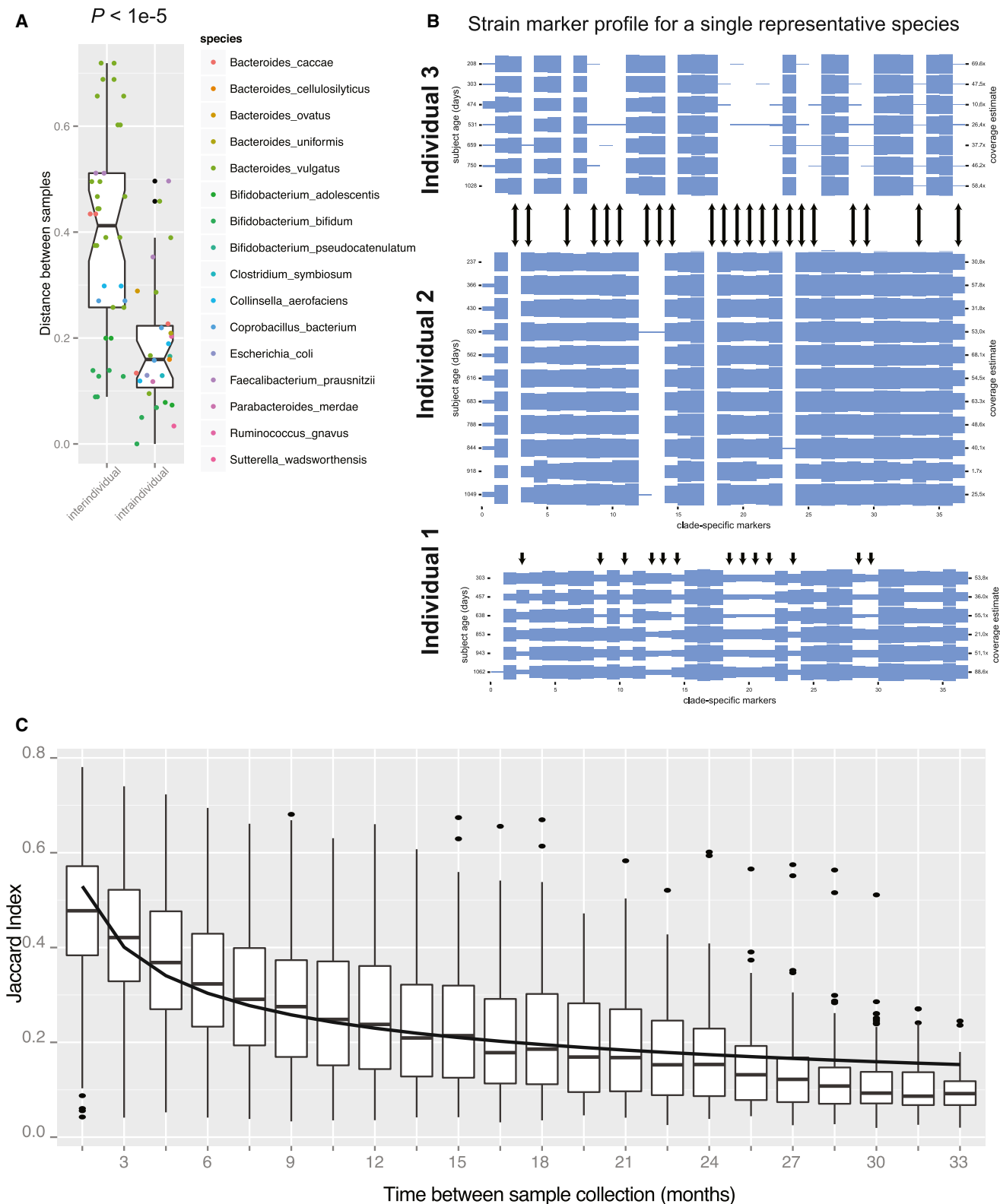


**Figure 4. Bacterial Strains Are Stably Maintained in the Infant Gut throughout Development**

(A) Distance between samples between subjects (interindividual) and within subjects (intraindividual) based on MetaPhlAn clade-specific strain marker analysis.

(legend continued on next page)



Additionally, we observed specific shifts in phylogenetic abundance with several other dietary parameters: eggs, barley, soy, and fish (nonsignificant) (Figure S3C). Notably, these shifts are less significant than those associated with geography or breast-feeding. Although we included antibiotic usage as a fixed effect for all MaAsLin analyses in this study, we did not have sufficient annotation on the timing of antibiotic usage to identify community shifts associated with antibiotics. We did not find differences in community composition between cesarean section versus vaginally delivered infants, perhaps because our cohort included only three cesarean-delivered subjects.

### Gut Microbiota Composition Distinguishes T1D Status

We next examined whether there were features of the microbial community that could distinguish T1D disease state. We assessed Chao1 alpha-diversity across time in nonconverter (not seroconverted), seroconverted (not diagnosed with T1D), and T1D cases (seroconverted subjects also diagnosed with T1D). We observed a pronounced flattening of the alpha-diversity in T1D subjects at a time when the gut communities of the nonconverter and seroconverted individuals continued to rise in alpha-diversity (Figure 5A). This result was significant by permutation test on subject labels ( $p < 0.025$ ; Figure S3D). Intriguingly, this divergence in alpha-diversity occurred after the time period in which most subjects seroconverted, but before the progressors presented with clinical disease.

To investigate the specific changes to the community that accounted for the decreased alpha-diversity in T1D subjects, we used MaAsLin analysis to focus on the time of the alpha-diversity divergence, after 600 days of age, and observed a number of significant alterations that distinguish T1D cases from nonconverters and seroconverters (Figure 5B). After correcting for potential confounding variables, we found that the drop in alpha-diversity in T1D cases could be accounted for by the relative overabundance of a few groups: *Blautia*, the Rikenellaceae, and the *Ruminococcus* and *Streptococcus* genera (not statistically significant). These groups of bacteria contain species that have been characterized as “pathobionts” (Chow and Mazmanian, 2009), which are members of the commensal microbiota that have the capacity to behave as pathogens. Our shotgun metagenomic sequencing revealed that specific pathobiont-like species within these groups, such as *Ruminococcus gnavus* and *Streptococcus infantarius*, showed a spike in relative abundance within the T1D cases at the time of alpha-diversity divergence (Figure 5C). Conversely, we saw a relative underabundance of a few groups of bacteria that are commonly depleted in the inflammatory state, namely the Lachnospiraceae and Veillonellaceae (not statistically significant) (Figure 5B), and metagenomic sequencing showed the complete absence of a number of these species, such as *Coprococcus eutactus* and *Dialister invisus*, in T1D cases (Figure 5C). Remarkably, seroconverters had an intermediate abundance of all of these groups

of organisms between nonconverters and T1D cases (Figure 5B), providing further evidence that this shift in microbiome composition is linked to the T1D disease state.

### Gut Microbial Gene Content Is Altered Prior to Clinical Onset of T1D

The NIH Human Microbiome Project has shown significant stability in microbial metabolic pathways across individuals despite high variability in taxonomic composition (Human Microbiome Project Consortium, 2012). We investigated whether changes in the abundance of specific metabolic pathways correlated with T1D status. After correcting for the effects of confounding variables such as age and diet using MaAsLin, we found significant shifts that occurred within T1D cases including an increase in the multiple sugar transport system, which is involved in the utilization of D-galactose, D-xylose, L-arabinose, D-glucose, and D-mannose, and a decrease in the biosynthesis of a number of amino acids (Figure 6A). A shift in functional potential from the synthesis of nutrients to the passive transporting-in of nutrients is characteristic of auxotrophic organisms. Auxotrophs thrive in inflammatory environments where dead tissue provides easy access to many nutrients that are less available in the healthy gut (Morgan et al., 2012). As was found for T1D-associated phylogenies, seroconverters had an intermediate level of abundance between nonconverters and T1D cases in metabolic pathway carriage (Figure 6A), and were more similar to nonconverters than T1D cases.

### Serum and Gut Lipids and Metabolites Relevant to Disease Are Correlated with T1D-Associated Microbial Taxa

The physiological effects of the gut microbiota extend beyond the gut; there is an interplay between both host and microbial enzymes and their metabolites which impacts host metabolism (Velagapudi et al., 2010) and mucosal immunity (Smith et al., 2013), as well as diseases including cardiovascular disease (Koeth et al., 2013; Wang et al., 2011). We assessed the correlation between serum polar metabolites and lipids with the gut microbiota. A Spearman correlation between absolute abundances of metabolites and microbial relative abundances yielded several metabolite-microbe clusters (Figure S4). Most significantly, we observed a clustering of triglycerides with a number of microbes, including a positive correlation between *Blautia* and long-chain triglycerides and *Ruminococcus* with short-chain triglycerides, and a negative correlation between *Veillonella* and short-chain triglycerides (Figure 6B). At the OTU level, we also observed correlations between members of these genera with branched-chain amino acids, specifically a positive correlation with *Blautia* and *Ruminococcus* members and a negative correlation with a *Veillonella* member (Figure 6C). Altered levels of serum triglycerides are a common feature of obesity and type 2 diabetes, and hypertriglyceridemia is

(B) Shown is the MetaPhlAn clade-specific strain marker profile for a single representative species (*Bacteroides ovatus*) for three separate individuals. Columns represent the 37 markers for this species, rows represent samples, and arrows indicate discordant markers between individuals 2 and 3 and indicate markers that undergo a change in abundance in individual 1.

(C) The Jaccard index (fraction of shared OTUs) between pairs of samples from the same individual within the indicated time window (i.e., 1.5 indicates 0–1.5 months, 6 indicates 4.5–6 months). The Jaccard index is shown for all pairs of samples across all subjects. A power-law curve was fitted to the medians of the boxplots (line). The box represents the first and third quartiles, and error bars indicate 95% confidence of median. See also Table S3.

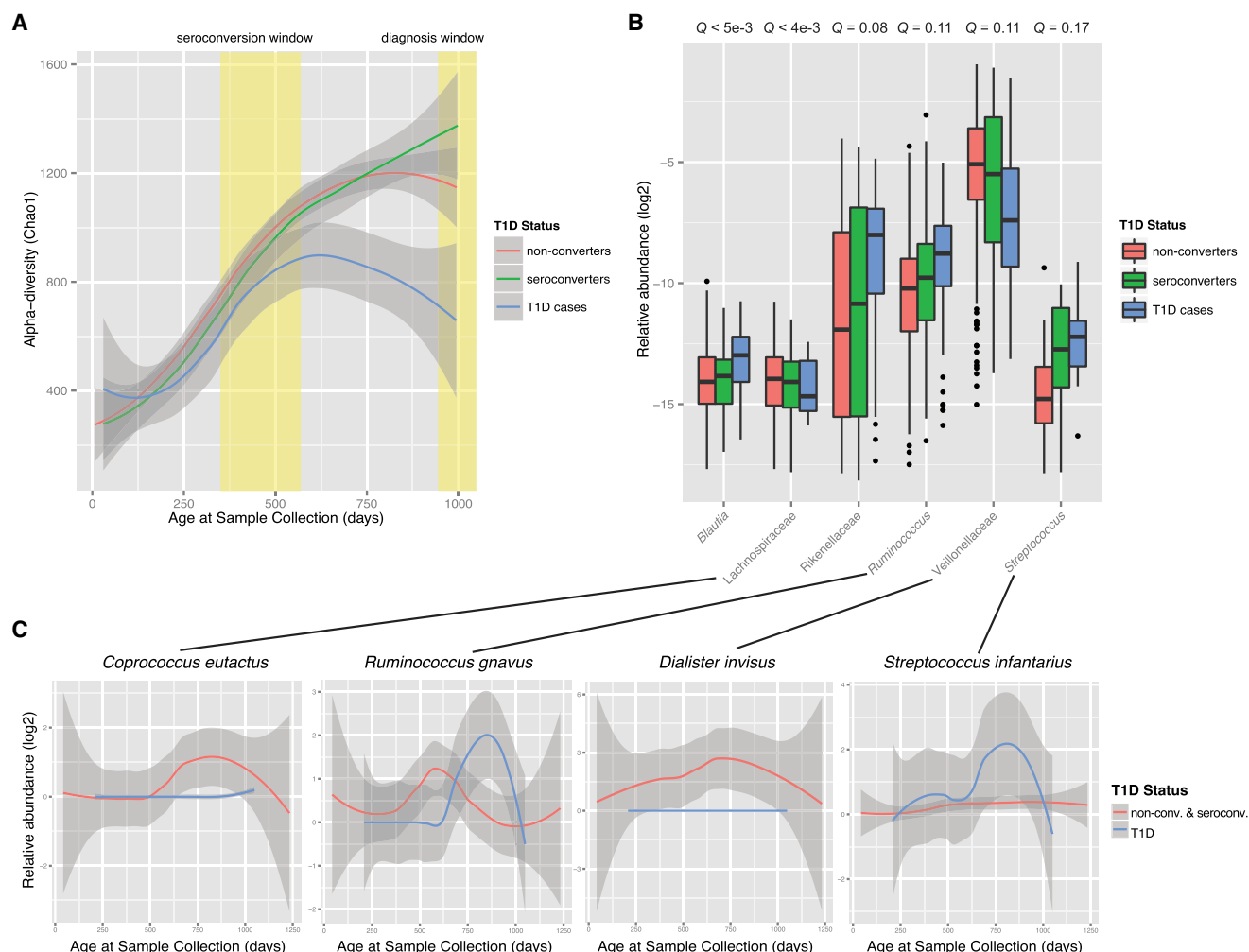


**Figure 5. The gut Microbiota Distinguishes Disease Status in T1D prior to Diagnosis**

(A) Plot of Chao1 alpha-diversity across time, represented as a smoothing spline with a 95% confidence interval (shaded region). The seroconversion window indicates the first and third quartiles for age at seroconversion for all seroconverted and T1D-diagnosed individuals, and the diagnosis window indicates the first quartile of time at T1D diagnosis (third quartile is 1,211 days).

(B) Abundances of the significantly differentially abundant taxa between T1D versus nonconverter and seroconverted individuals, including only samples between the seroconversion and diagnosis windows. FDR-corrected p values (Q values) were calculated using MaAsLin. The box represents the first and third quartiles; error bars indicate 95% confidence of median.

(C) Plots of the relative abundance of representative species from shotgun metagenomics data, represented as a smoothing spline with a 95% confidence interval (shaded region). See also Figures S3 and S5.

associated with poor glycemic control and nephropathy in T1D (Alcantara et al., 2011; Vergès, 2009). Additionally, elevated branched-chain amino acids have been shown in both patients (Vannini et al., 1982) and in mouse models (Mochida et al., 2011; Sailer et al., 2013) of diabetes, as well as preceding islet autoimmunity in children who later progress to T1D (Orešić et al., 2008). We found a positive correlation between *Blautia* and *Ruminococcus*, both of which have increased abundance in T1D cases, with triglycerides and branched-chain amino acids, possibly indicating that these microbe-metabolite relationships cooperatively impact T1D progression.

To conduct an integrative analysis of the correlations that exist between the gut microbiome and the gut (stool) metabolome, we performed penalized canonical correlation analysis

(Figures 6D; see Experimental Procedures). This analysis identified a canonical variate that associates increased *Ruminococcus* and decreased *Veillonella* abundance with increased sphingomyelin and decreased lithocholic acid levels (Pearson R = 0.61; Q = 0.03). Sphingomyelin is a member of the sphingolipids, which inhibit intestinal natural killer T cell function and protect against oxazolone-induced colitis (An et al., 2014). Lithocholic acid, similar to deoxycholic acid, is a secondary bile acid that promotes intestinal inflammation by eliciting reactive oxygen and nitrogen species and activating NF- $\kappa$ B activity in intestinal epithelial cells (Lee et al., 2004; Mühlbauer et al., 2004; Payne et al., 2007; Sears and Garrett, 2014; Da Silva et al., 2012). Although the alterations to the microbiota that we observed may be related to impaired glucose metabolism in

the prediabetic stage, these results suggest that the T1D-associated microbiota that becomes established prior to disease onset may actively promote a metabolic environment in the gut that is permissive to inflammation and promotes pathogenesis.

## DISCUSSION

To identify and understand alterations to the gut microbial community composition that may contribute to childhood disease, we must first investigate the normal dynamics of the community in the developing infant. Here, we identify a set of principles that describe microbiome development in the infant gut. We note as a caveat that all children in this cohort carry T1D-predisposing HLA alleles and are restricted to the countries of Finland and Estonia, and are therefore not necessarily representative of genetically “normal” infants in other regions of the world. First, although there is great variation in overall taxonomic composition between and within individuals over time, there is significantly less variation in the metabolic composition of the microbiome, and almost no variation in its metabolic pathway coding potential. This result provides a variation on the finding made in the NIH Human Microbiome Project regarding the stability of metabolic pathways in the microbiome between healthy adults (Human Microbiome Project Consortium, 2012) and suggests that the relative proportions of bacterial functional pathways remains the same from soon after birth until 3 years of age. We speculate that because the taxonomic composition of the microbiome stabilizes at approximately 3 years, functional pathways likely remain stable for long after this age as well.

Second, we identified shared taxonomic trajectories, remarkably consistent across individuals, that indicate general changes in abundance, the timing of these shifts, and the relationships between community members. For example, we saw a strong positive correlation between the Lachnospiraceae and Rumino-coccaceae, both Gram-positive anaerobes that are inversely correlated with the Enterobacteriaceae, Gram-negative aerobes. In turn, the Enterobacteriaceae are positively correlated with the Bifidobacteriaceae, which decrease in abundances after cessation of breastfeeding. Although there are many exceptions to general trends, we observed a decrease in Gram-negative bacteria over time, and found that early colonizers are aerobic, whereas later colonizers tend to be anaerobic. Similar trends have been observed previously (Dominguez-Bello et al., 2010; Koenig et al., 2011; Palmer et al., 2007); however, the significantly higher density of sampling, size, and longitudinal nature of our cohort provide a high-resolution map of these dynamics and demonstrate how universal they are across infants.

Third, we demonstrated a surprising stability in the maintenance of specific strains through time. Although the strain composition is quite distinct between individuals, as expected, the strain composition within an individual remains essentially constant throughout infancy for almost all individuals and almost all species that have sufficiently high abundance for stability analysis.

In addition to shared trends, we identified aspects of infant gut microbiome development that are unique to the T1D state. We observed a significant alteration in the structure of the

T1D-associated gut microbiome: a relative 25% reduction in alpha-diversity compared to nonconverters and seroconverters, associated with shifts in both microbial phylogenetic and metabolic pathways. Importantly, this shift is seen in children who are diagnosed with T1D within the study time frame, but not in seroconverters without disease. Although the probability of progression to T1D after positivity for two islet autoantibodies is greater than 80% after follow-up for 15 years (Ziegler et al., 2013), there is significant variability in when progression occurs, ranging from weeks to more than two decades (Knip et al., 2010), and the factors contributing to this variability are not well understood. The logistics of densely sampling a large cohort of individuals through T1D diagnosis limits the time frame of such a study, and we therefore are reporting on a special subset of T1D cases with early onset diabetes (EOD) (Harjutsalo et al., 2013). We provide evidence that pronounced alterations occur in the gut microbiome that precede overt disease.

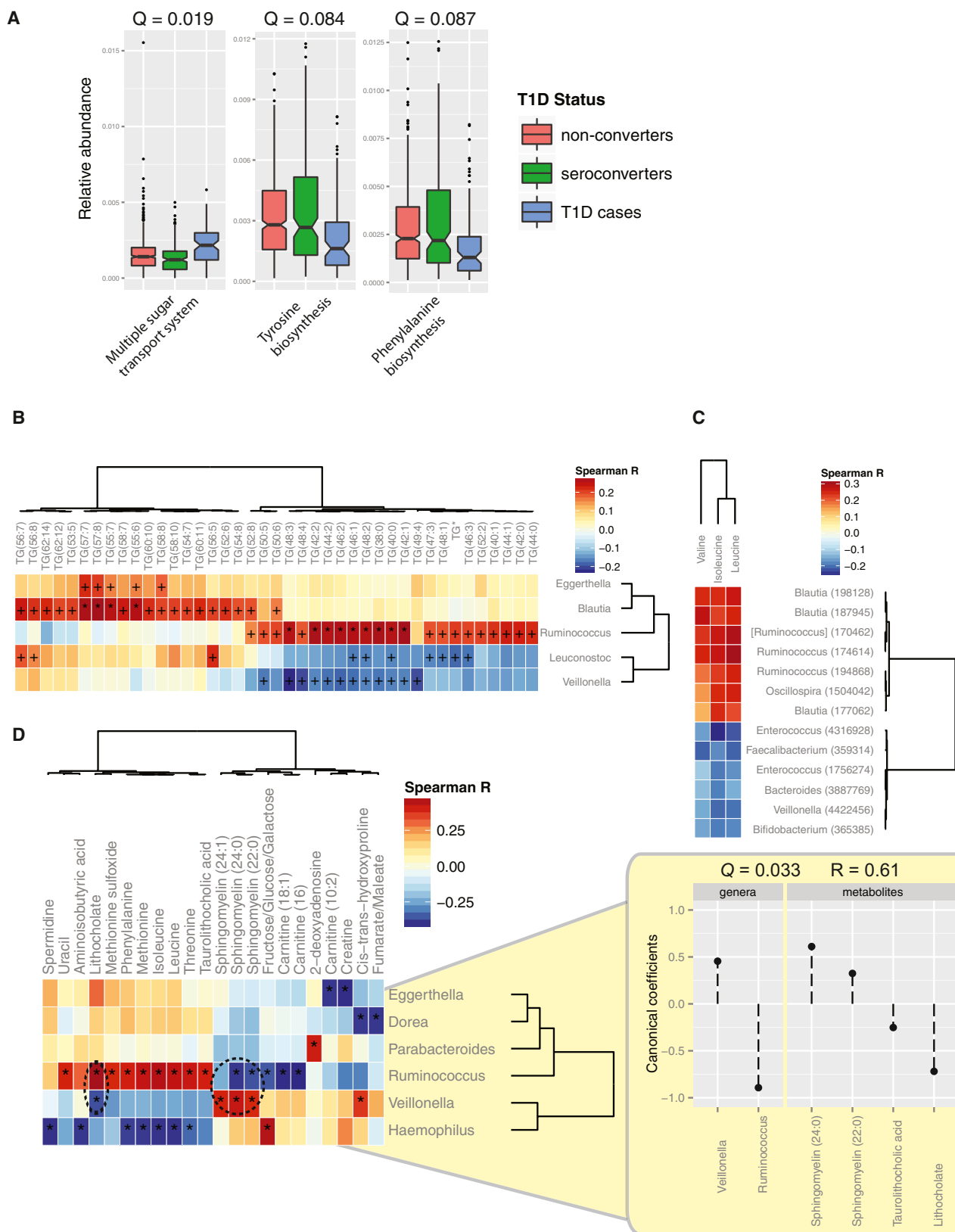
Although previous studies of human cohorts have been constrained by the availability of sufficient longitudinal samples and subject groupings that distinguished seroconverting non-progressors from T1D progressors, they have shown a decreased microbial diversity in children with long-lasting  $\beta$  cell autoimmunity and in progressors to clinical T1D compared to nonseroconverted controls (Brown et al., 2011; Giongo et al., 2011; de Goffau et al., 2013). Here, we demonstrated that this shift occurs prior to onset of disease but after seroconversion, and identified that it is specific to T1D progressors and not seen in seroconverters without disease. Decreased microbial diversity is a hallmark of dysbiosis and has been observed in obesity (Turnbaugh et al., 2009), inflammatory bowel disease (Manichanh et al., 2012), and *Clostridium difficile*-associated diarrhea (Chang et al., 2008). A recent study showed that a failure to establish a critical level of diversity in the gut microbiota of developing mice resulted in long-term increases in IgE levels, thus predisposing mice to immune-mediated disorders (Cahenzli et al., 2013). Decreased diversity results from the blooming of a small subset of the community that crowds out other community members.

Additionally, we find higher levels of human  $\beta$ -defensin 2 (hBD2) in early samples of children who develop T1D (Figure S5). hBD2 is an antimicrobial product induced by colonic epithelial cells during inflammation (O’Neil et al., 1999; Wehkamp et al., 2005); therefore, this result is supportive of increased intestinal inflammation in the cohort of children who go on to develop T1D. It has been proposed that an aberrant gut microbiota, a permeable intestinal mucosal barrier, and an altered mucosal immune response collectively contribute to the development of T1D (Vaarala et al., 2008). Our results prompt further functional studies to determine whether the proinflammatory microbiome we observe to bloom prior to clinical disease onset may take advantage of or drive increased intestinal permeability and intestinal inflammation to contribute to T1D pathogenesis.

## EXPERIMENTAL PROCEDURES

### Study Cohort

Please see Supplemental Experimental Procedures for cohort recruitment and sample and information collection details.



(legend on next page)

### Stool Sample Collection and DNA Extraction

Stool samples were collected by participants' parents and stored in the household freezer ( $-20^{\circ}\text{C}$ ) until the next visit to the local study center; samples were then shipped on dry ice to the DIABIMMUNE Core Laboratory. The samples were then stored at  $-80^{\circ}\text{C}$  until shipping to the Broad Institute for DNA extraction. DNA extractions from stool were carried out using the QIAamp DNA Stool Mini Kit (QIAGEN, Inc., Valencia, CA, USA).

### Sequencing and Analysis of the 16S Gene and Shotgun Metagenomics

16S sequencing and metagenomics was performed essentially as previously described (Gevers et al., 2014). Additional details are available in the [Supplemental Experimental Procedures](#).

### Phylogenetic Abundance Trajectory Network Analysis

Analysis was limited to the 29 individuals without T1D. Samples from the 16S OTU abundance table were binned into 20 time windows from 50 to 1,100 days, selecting the nearest sample in time for each bin. Read counts from the 16S OTU abundance table were collapsed at each phylogenetic level, from phylum to genus, and compositionally normalized such that the abundance in each sample sums to one. At each phylogenetic level, on a per-individual basis, the correlation between every clade-clade pair was performed in CCPEPE (<http://huttenhower.sph.harvard.edu/ccpepe>; previously known as "ReBoot"; Faust et al., 2012). The default similarity metric, Spearman, was used. Only correlations with a Q value  $< 0.1$  were included in analysis. For each filtered clade-clade pair, the Z statistic was summed across all 29 individuals, and only pairs with a cumulative absolute Z statistic value of  $>20$  were carried forward, as this was a conservative cutoff for consistent correlations across many subjects. The cumulative Z statistic was scaled without centering using the R "scale" function and then visualized as a network diagram on Cytoscape.

### Human $\beta$ -Defensin 2 Measurement from Stool Samples

Frozen stool samples were thawed at room temperature immediately prior to analysis. Fecal human  $\beta$ -defensin 2 (hBD2) levels were determined by enzyme linked immunoabsorbent assay (ELISA) using the  $\beta$ -defensin 2 ELISA Kit (Imundiagnostik, Bensheim, Germany) adapted for fecal samples as described previously (Kapel et al., 1999).

### Metabolomics and Lipidomics Profiling from Serum and Stool

Please see [Supplemental Experimental Procedures](#) for detailed metabolomics and lipidomics protocols and sample handling information.

### Community Stability Analysis

The Jaccard index for a given sample pair is defined as  $(\text{sample A} \cap \text{sample B}) / (\text{sample A} \cup \text{sample B})$  and calculated using the compositionally normalized 16S OTU table. On a per-individual basis, the Jaccard index was calculated for all samples that fell into time windows of 1.5 months in length, beginning at 0–1.5 months up to 31.5–33 months.

### MaAsLin Analysis

MaAsLin analysis was performed using default parameters (<http://huttenhower.sph.harvard.edu/maaslin>). Subject ID was used as a random effect. The following variables were used as fixed effects for every analysis, in addition to the variable of interest: T1D status, age, gender, country, delivery mode, time and name of antibiotic exposure, total reads per sample, sequencing batch ID, breastfeeding (on/off), solid food (on/off), eggs (on/off),

fish (on/off), soy products (on/off), rye (on/off), barley (on/off), and buckwheat and millet (on/off).

### Alpha-Diversity

Alpha-diversity analysis of the 16S OTU table was performed in QIIME 1.5.0 (Caporaso et al., 2010) with the `alpha_diversity.py` script using the "chao1" metric and default parameters. Permutation-based analysis of significance was performed on a per-subject basis by shuffling the T1D subject label through all individuals and recalculating the difference in Chao1 mean between T1D subjects versus control and seroconverted subjects. Ten thousand permutations were performed.

### SUPPLEMENTAL INFORMATION

Supplemental Information includes Supplemental Experimental Procedures, five figures, and three tables and can be found with this article at <http://dx.doi.org/10.1016/j.chom.2015.01.001>.

### CONSORTIA

The members of the DIABIMMUNE Study Group are Mikael Knip, Katriina Koski, Matti Koski, Taina Härkönen, Samppa Ryhänen, Heli Siljander, AnuMaaria Hämäläinen, Anne Ormiston, Aleksandr Peet, Vallo Tillmann, Valentina Ulich, Elena Kuzmicheva, Sergei Mokurov, Svetlana Markova, Svetlana Pylova, Marina Isakova, Elena Shakurova, Vladimir Petrov, Natalya V. Dorshakova, Tatyana Karapetyan, Tatyana Varlamova, Jorma Ilonen, Minna Kiviniemi, Kristi Alnek, Helis Janson, Raivo Uibo, Tiit Salum, Erika von Mutius, Juliane Weber, Helena Ahlfors, Henna Kallionpää, Essi Laajala, Riitta Lahtesmaa, Harri Lähdesmäki, Robert Molder, Viveka Öling, Janne Nieminen, Terhi Ruohutla, Outi Vaarala, Hanna Honkanen, Heikki Hyöty, Anita Kondrashova, Sami Oikarinen, Hermie J.M. Harmsen, Marcus C. De Goffau, Gjal Welling, Kirsi Alahuhta, Tuuli Korhonen, Suvi M. Virtanen, and Taina Öhman.

### ACKNOWLEDGMENTS

We thank Tiffany Poon (Broad Institute) for sample, sequencing, and data coordination; Timothy L. Tickle, Emma Schwager, and Xochitl C. Morgan (Harvard School of Public Health) for assistance with statistical analysis and helpful discussions; Natalia Nedelsky (MGH) for editorial assistance; Niina Lietzen, Leena Öhrnberg, Anna-Liisa Ruskeepää, and Heli Nygren (VTT Technical Research Centre of Finland) for assistance in metabolomics analysis; and Katriina Koski and Matti Koski (Institute of Clinical Medicine, University of Helsinki) for the coordination and data base work of the DIABIMMUNE Study. This work was supported by the European Union Seventh Framework Programme FP7/2007–2013 under grant agreement number 202063; Juvenile Diabetes Research Foundation grants 17–2011–529 and 17–2014–305; The Academy of Finland Centre of Excellence in Molecular Systems Immunology and Physiology Research grant Decision number 250114, 2012–2017; and National Institutes of Health P30 DK043351 and U54 DK102557. Outi Vaarala was an employee of AstraZeneca Research & Development beginning August 1, 2014.

Received: August 25, 2014

Revised: November 5, 2014

Accepted: December 23, 2014

Published: February 5, 2015; corrected online: June 25, 2016

### Figure 6. Gut Microbial Gene Content and Serum and Gut Metabolites Are Altered prior to T1D Onset

(A) Abundances of the significantly differentially abundant KEGG modules between T1D versus seroconverted individuals, including only samples between the seroconversion and diagnosis windows. FDR-corrected p values (Q values) were calculated using MaAsLin. The box represents the first and third quartiles; error bars indicate 95% confidence of median.

(B and C) (B) Spearman correlations between serum triglycerides and the five most-correlated genera, and (C) between the branched-chain amino acids and OTUs using a cutoff of  $p < 0.001$ . +, correlations with  $p < 0.05$ ; \*, correlations with  $Q < 0.05$ . "TG\*" represents TG(14:0/18:1/18:1) + TG(16:0/16:1/18:1).

(D) Spearman correlations between stool metabolites and lipids and the most-correlated genera. Coefficients of the canonical variates including *Ruminococcus*, *Veillonella*, and correlated metabolites obtained using penalized canonical correlation analysis. See also [Figure S4](#).



## REFERENCES

- Aagaard, K., Ma, J., Antony, K.M., Ganu, R., Petrosino, J., and Versalovic, J. (2014). The placenta harbors a unique microbiome. *Sci. Transl. Med.* **6**, 237ra65.
- Abubucker, S., Segata, N., Goll, J., Schubert, A.M., Izard, J., Cantarel, B.L., Rodriguez-Mueller, B., Zucker, J., Thiagarajan, M., Henrissat, B., et al. (2012). Metabolic reconstruction for metagenomic data and its application to the human microbiome. *PLoS Comput. Biol.* **8**, e1002358.
- Achenbach, P., Bonifacio, E., Koczwara, K., and Ziegler, A.-G. (2005). Natural history of type 1 diabetes. *Diabetes* **54** (Suppl 2), S25–S31.
- Alcantara, L.M., Silveira, N.E., Dantas, J.R., Araujo, P.B., de Oliveira, M.M., Milech, A., Zajdenverg, L., Rodacki, M., and de Oliveira, J.E. (2011). Low triglyceride levels are associated with a better metabolic control in patients with type 1 diabetes. *Diabetol. Metab. Syndr.* **3**, 22.
- An, D., Oh, S.F., Olszak, T., Neves, J.F., Avci, F.Y., Ertürk-Hasdemir, D., Lu, X., Zeissig, S., Blumberg, R.S., and Kasper, D.L. (2014). Sphingolipids from a symbiotic microbe regulate homeostasis of host intestinal natural killer T cells. *Cell* **156**, 123–133.
- Brown, C.T., Davis-Richardson, A.G., Giongo, A., Gano, K.A., Crabb, D.B., Mukherjee, N., Casella, G., Drew, J.C., Ilonen, J., Knip, M., et al. (2011). Gut microbiome metagenomics analysis suggests a functional model for the development of autoimmunity for type 1 diabetes. *PLoS ONE* **6**, e25792.
- Cahenzli, J., Köller, Y., Wyss, M., Geuking, M.B., and McCoy, K.D. (2013). Intestinal microbial diversity during early-life colonization shapes long-term IgE levels. *Cell Host Microbe* **14**, 559–570.
- Caporaso, J.G., Kuczynski, J., Stombaugh, J., Bittinger, K., Bushman, F.D., Costello, E.K., Fierer, N., Peña, A.G., Goodrich, J.K., Gordon, J.I., et al. (2010). QIIME allows analysis of high-throughput community sequencing data. *Nat. Methods* **7**, 335–336.
- Caporaso, J.G., Lauber, C.L., Walters, W.A., Berg-Lyons, D., Huntley, J., Fierer, N., Owens, S.M., Betley, J., Fraser, L., Bauer, M., et al. (2012). Ultra-high-throughput microbial community analysis on the Illumina HiSeq and MiSeq platforms. *ISME J.* **6**, 1621–1624.
- Chang, J.Y., Antonopoulos, D.A., Kalra, A., Tonelli, A., Khalife, W.T., Schmidt, T.M., and Young, V.B. (2008). Decreased diversity of the fecal Microbiome in recurrent *Clostridium difficile*-associated diarrhea. *J. Infect. Dis.* **197**, 435–438.
- Cho, I., Yamanishi, S., Cox, L., Methé, B.A., Zavadil, J., Li, K., Gao, Z., Mahana, D., Raju, K., Teitler, I., et al. (2012). Antibiotics in early life alter the murine colonic microbiome and adiposity. *Nature* **488**, 621–626.
- Chow, J., and Mazmanian, S.K. (2009). Getting the bugs out of the immune system: do bacterial microbiota “fix” intestinal T cell responses? *Cell Host Microbe* **5**, 8–12.
- Cox, L.M., Yamanishi, S., Sohn, J., Alekseyenko, A.V., Leung, J.M., Cho, I., Kim, S.G., Li, H., Gao, Z., Mahana, D., et al. (2014). Altering the intestinal microbiota during a critical developmental window has lasting metabolic consequences. *Cell* **158**, 705–721.
- Da Silva, M., Jaggars, G.K., Verstraeten, S.V., Erleijman, A.G., Fraga, C.G., and Oteiza, P.I. (2012). Large procyanidins prevent bile-acid-induced oxidant production and membrane-initiated ERK1/2, p38, and Akt activation in Caco-2 cells. *Free Radic. Biol. Med.* **52**, 151–159.
- de Goffau, M.C., Luopajarvi, K., Knip, M., Ilonen, J., Ruotula, T., Härkönen, T., Orivuori, L., Hakala, S., Welling, G.W., Harmsen, H.J., and Vaarala, O. (2013). Fecal microbiota composition differs between children with  $\beta$ -cell autoimmunity and those without. *Diabetes* **62**, 1238–1244.
- Dominguez-Bello, M.G., Costello, E.K., Contreras, M., Magris, M., Hidalgo, G., Fierer, N., and Knight, R. (2010). Delivery mode shapes the acquisition and structure of the initial microbiota across multiple body habitats in newborns. *Proc. Natl. Acad. Sci. USA* **107**, 11971–11975.
- Faith, J.J., Guruge, J.L., Charbonneau, M., Subramanian, S., Seedorf, H., Goodman, A.L., Clemente, J.C., Knight, R., Heath, A.C., Leibel, R.L., et al. (2013). The long-term stability of the human gut microbiota. *Science* **341**, 1237439.
- Faust, K., Sathirapongsasuti, J.F., Izard, J., Segata, N., Gevers, D., Raes, J., and Huttenhower, C. (2012). Microbial co-occurrence relationships in the human microbiome. *PLoS Comput. Biol.* **8**, e1002606.
- Gevers, D., Kugathasan, S., Denson, L.A., Vázquez-Baeza, Y., Van Treuren, W., Ren, B., Schwager, E., Knights, D., Song, S.J., Yassour, M., et al. (2014). The treatment-naïve microbiome in new-onset Crohn’s disease. *Cell Host Microbe* **15**, 382–392.
- Giongo, A., Gano, K.A., Crabb, D.B., Mukherjee, N., Novelo, L.L., Casella, G., Drew, J.C., Ilonen, J., Knip, M., Hyöty, H., et al. (2011). Toward defining the autoimmune microbiome for type 1 diabetes. *ISME J.* **5**, 82–91.
- Harjutsalo, V., Sjöberg, L., and Tuomilehto, J. (2008). Time trends in the incidence of type 1 diabetes in Finnish children: a cohort study. *Lancet* **371**, 1777–1782.
- Harjutsalo, V., Sund, R., Knip, M., and Groop, P.-H. (2013). Incidence of type 1 diabetes in Finland. *JAMA* **310**, 427–428.
- Human Microbiome Project Consortium (2012). Structure, function and diversity of the healthy human microbiome. *Nature* **486**, 207–214.
- Kapel, N., Matarazzo, P., Haouchine, D., Abiola, N., Guérin, S., Magne, D., Gobert, J.G., and Dupont, C. (1999). Fecal tumor necrosis factor alpha, eosinophil cationic protein and IgE levels in infants with cow’s milk allergy and gastrointestinal manifestations. *Clin. Chem. Lab. Med.* **37**, 29–32.
- Knip, M., Veijola, R., Virtanen, S.M., Hyöty, H., Vaarala, O., and Akerblom, H.K. (2005). Environmental triggers and determinants of type 1 diabetes. *Diabetes* **54** (Suppl 2), S125–S136.
- Knip, M., Korhonen, S., Kulmala, P., Veijola, R., Reunanen, A., Raitakari, O.T., Viikari, J., and Akerblom, H.K. (2010). Prediction of type 1 diabetes in the general population. *Diabetes Care* **33**, 1206–1212.
- Koenig, J.E., Spor, A., Scalfone, N., Fricker, A.D., Stombaugh, J., Knight, R., Angenent, L.T., and Ley, R.E. (2011). Succession of microbial consortia in the developing infant gut microbiome. *Proc. Natl. Acad. Sci. USA* **108** (Suppl 1), 4578–4585.
- Koeth, R.A., Wang, Z., Levison, B.S., Buffa, J.A., Org, E., Sheehy, B.T., Britt, E.B., Fu, X., Wu, Y., Li, L., et al. (2013). Intestinal microbiota metabolism of L-carnitine, a nutrient in red meat, promotes atherosclerosis. *Nat. Med.* **19**, 576–585.
- Langille, M.G.I., Zaneveld, J., Caporaso, J.G., McDonald, D., Knights, D., Reyes, J.A., Clemente, J.C., Burkepile, D.E., Vega Thurber, R.L., Knight, R., et al. (2013). Predictive functional profiling of microbial communities using 16S rRNA marker gene sequences. *Nat. Biotechnol.* **31**, 814–821.
- Lee, D.K., Park, S.Y., Baik, S.K., Kwon, S.O., Chung, J.M., Oh, E.-S., and Kim, H.S. (2004). [Deoxycholic acid-induced signal transduction in HT-29 cells: role of NF- $\kappa$ B and interleukin-8]. *Korean J. Gastroenterol.* **43**, 176–185.
- Manichanh, C., Borruel, N., Casellas, F., and Guarner, F. (2012). The gut microbiota in IBD. *Nat. Rev. Gastroenterol. Hepatol.* **9**, 599–608.
- Mochida, T., Tanaka, T., Shiraki, Y., Tajiri, H., Matsumoto, S., Shimbo, K., Ando, T., Nakamura, K., Okamoto, M., and Endo, F. (2011). Time-dependent changes in the plasma amino acid concentration in diabetes mellitus. *Mol. Genet. Metab.* **103**, 406–409.
- Morgan, X.C., Tickle, T.L., Sokol, H., Gevers, D., Devaney, K.L., Ward, D.V., Reyes, J.A., Shah, S.A., LeLeiko, N., Snapper, S.B., et al. (2012). Dysfunction of the intestinal microbiome in inflammatory bowel disease and treatment. *Genome Biol.* **13**, R79.
- Mühlbauer, M., Allard, B., Bosserhoff, A.K., Kiessling, S., Herfarth, H., Rogler, G., Schölmerich, J., Jobin, C., and Hellerbrand, C. (2004). Differential effects of deoxycholic acid and taurodeoxycholic acid on NF- $\kappa$ B signal transduction and IL-8 gene expression in colonic epithelial cells. *Am. J. Physiol. Gastrointest. Liver Physiol.* **286**, G1000–G1008.
- O’Neil, D.A., Porter, E.M., Elewaut, D., Anderson, G.M., Eckmann, L., Ganz, T., and Kagnoff, M.F. (1999). Expression and regulation of the human beta-defensins hBD-1 and hBD-2 in intestinal epithelium. *J. Immunol.* **163**, 6718–6724.
- Orešić, M., Simell, S., Sysi-Aho, M., Näntö-Salonen, K., Seppänen-Laakso, T., Parikka, V., Katajamaa, M., Hekkala, A., Mattila, I., Keskinen, P., et al. (2008). Dysregulation of lipid and amino acid metabolism precedes islet autoimmunity in children who later progress to type 1 diabetes. *J. Exp. Med.* **205**, 2975–2984.



- Palmer, C., Bik, E.M., DiGiulio, D.B., Relman, D.A., and Brown, P.O. (2007). Development of the human infant intestinal microbiota. *PLoS Biol.* 5, e177.
- Payne, C.M., Weber, C., Crowley-Skillicorn, C., Dvorak, K., Bernstein, H., Bernstein, C., Holubec, H., Dvorakova, B., and Garewal, H. (2007). Deoxycholate induces mitochondrial oxidative stress and activates NF-kappaB through multiple mechanisms in HCT-116 colon epithelial cells. *Carcinogenesis* 28, 215–222.
- Sailer, M., Dahlhoff, C., Giesbertz, P., Eidens, M.K., de Wit, N., Rubio-Aliaga, I., Boekschoten, M.V., Müller, M., and Daniel, H. (2013). Increased plasma citrulline in mice marks diet-induced obesity and may predict the development of the metabolic syndrome. *PLoS ONE* 8, e63950.
- Sears, C.L., and Garrett, W.S. (2014). Microbes, microbiota, and colon cancer. *Cell Host Microbe* 15, 317–328.
- Segata, N., Waldron, L., Ballarini, A., Narasimhan, V., Jousson, O., and Huttenhower, C. (2012). Metagenomic microbial community profiling using unique clade-specific marker genes. *Nat. Methods* 9, 811–814.
- Smith, P.M., Howitt, M.R., Panikov, N., Michaud, M., Gallini, C.A., Bohlooly-Y, M., Glickman, J.N., and Garrett, W.S. (2013). The microbial metabolites, short-chain fatty acids, regulate colonic Treg cell homeostasis. *Science* 341, 569–573.
- Subramanian, S., Huq, S., Yatsunenko, T., Haque, R., Mahfuz, M., Alam, M.A., Benezra, A., DeStefano, J., Meier, M.F., Muegge, B.D., et al. (2014). Persistent gut microbiota immaturity in malnourished Bangladeshi children. *Nature* 510, 417–421.
- Turnbaugh, P.J., Hamady, M., Yatsunenko, T., Cantarel, B.L., Duncan, A., Ley, R.E., Sogin, M.L., Jones, W.J., Roe, B.A., Affourtit, J.P., et al. (2009). A core gut microbiome in obese and lean twins. *Nature* 457, 480–484.
- Vaarala, O., Atkinson, M.A., and Neu, J. (2008). The “perfect storm” for type 1 diabetes: the complex interplay between intestinal microbiota, gut permeability, and mucosal immunity. *Diabetes* 57, 2555–2562.
- Vannini, P., Marchesini, G., Forlani, G., Angiolini, A., Ciavarella, A., Zoli, M., and Pisi, E. (1982). Branched-chain amino acids and alanine as indices of the metabolic control in type 1 (insulin-dependent) and type 2 (non-insulin-dependent) diabetic patients. *Diabetologia* 22, 217–219.
- Velagapudi, V.R., Hezaveh, R., Reigstad, C.S., Gopalacharyulu, P., Yetukuri, L., Islam, S., Felin, J., Perkins, R., Borén, J., Oresic, M., and Bäckhed, F. (2010). The gut microbiota modulates host energy and lipid metabolism in mice. *J. Lipid Res.* 51, 1101–1112.
- Vergès, B. (2009). Lipid disorders in type 1 diabetes. *Diabetes Metab.* 35, 353–360.
- Wang, Z., Klipfelf, E., Bennett, B.J., Koeth, R., Levison, B.S., Dugar, B., Feldstein, A.E., Britt, E.B., Fu, X., Chung, Y.-M., et al. (2011). Gut flora metabolism of phosphatidylcholine promotes cardiovascular disease. *Nature* 472, 57–63.
- Wehkamp, J., Schmid, M., Fellermann, K., and Stange, E.F. (2005). Defensin deficiency, intestinal microbes, and the clinical phenotypes of Crohn's disease. *J. Leukoc. Biol.* 77, 460–465.
- Wen, L., Ley, R.E., Volchkov, P.Y., Stranges, P.B., Avanesyan, L., Stonebraker, A.C., Hu, C., Wong, F.S., Szot, G.L., Bluestone, J.A., et al. (2008). Innate immunity and intestinal microbiota in the development of Type 1 diabetes. *Nature* 455, 1109–1113.
- Yatsunenko, T., Rey, F.E., Manary, M.J., Trehan, I., Dominguez-Bello, M.G., Contreras, M., Magris, M., Hidalgo, G., Baldassano, R.N., Anokhin, A.P., et al. (2012). Human gut microbiome viewed across age and geography. *Nature* 486, 222–227.
- Ziegler, A.G., Rewers, M., Simell, O., Simell, T., Lempainen, J., Steck, A., Winkler, C., Ilonen, J., Veijola, R., Knip, M., et al. (2013). Seroconversion to multiple islet autoantibodies and risk of progression to diabetes in children. *JAMA* 309, 2473–2479.